

## Swarmalators on a ring with distributed couplings

Kevin O’Keeffe<sup>1</sup> and Hyunsuk Hong<sup>2,3,\*</sup>

<sup>1</sup>*Senseable City Lab, Massachusetts Institute of Technology, Cambridge, Massachusetts 02139, USA*

<sup>2</sup>*Department of Physics and Research Institute of Physics and Chemistry, Jeonbuk National University, Jeonju 54896, Korea*

<sup>3</sup>*School of Physics, Korea Institute for Advanced Study, Seoul 02455, Korea*



(Received 18 April 2022; accepted 25 May 2022; published 16 June 2022)

We study a simple model of identical “swarmalators,” generalizations of phase oscillators that swarm through space. We confine the movements to a one-dimensional (1D) ring and consider distributed (nonidentical) couplings; the combination of these two effects captures an aspect of the more realistic two-dimensional swarmalator model. We discover several collective states which we describe analytically. These states imitate the behavior of vinegar eels, catalytic microswimmers, and other swarmalators which move on quasi-1D rings.

DOI: [10.1103/PhysRevE.105.064208](https://doi.org/10.1103/PhysRevE.105.064208)

### I. INTRODUCTION

An interplay between sync [1–3] (self-organization in time) and swarming [4,5] (self-organization in space) crops up everywhere in nature, from biological microswimmers [6–11] and chemical nanomotors [12–19] to magnetic domains walls [20,21] and robotic swarms [22–24]. Yet little is known about this dual form of self-organization from a theoretical perspective. Tanaka gave the first mathematical treatment of it by deriving a model of chemotactic oscillators, oscillators which are pushed around by chemical gradients which in turn influence the oscillators’ phases. [25–28]. Later O’Keeffe *et al.* introduced a phenomenological model of “swarmalators” [29], short for swarming oscillators, which mimics various real-world systems [14,22,23]. Several researchers are now further exploring swarmalators [30–41].

The physics of the swarmalator model [29] is not yet understood. Varying one parameter produces five collective states (Fig. 1); the three static states [Figs. 1(a)–1(c)] have been analyzed [29], but the two dynamical states [Figs. 1(d) and 1(e)] remain murky—What is the nature of the flow in the vortex-like active phase wave [Fig. 1(e)]? Does it imitate the flow in vortices of Janus crystals and sperm [7,42]? What determines the number of minivortices in the splintered phase wave [Fig. 1(d)]? Do they mimic the rotating flocks seen in active fluids [14]? The stabilities and bifurcations of *all* states are also a mystery. Figure 2 illustrates the bifurcation structure by plotting the order parameters  $S_{\pm} e^{i\Phi_{\pm}} := N^{-1} \sum_j e^{i(\phi_j - \theta_j)}$  (where  $\phi, \theta$  are the angular position and phase; see the Appendix) vs the phase coupling  $K$ . At an unknown  $K_1$ ,  $S_+$  jumps from 0 as the async state transitions to the active phase wave. At a later  $K_2$ ,  $S_+$  begins to decline as the splintered phase wave is born. Like the old puzzles about the Kuramoto model [2,43–46], the bifurcations of the swarmalator model “cry out for explanation” [43,47].

This work is a single step in a longer journey to provide such an explanation [47,48]. Our dream is to repurpose the

tools from the sync world (Kuramoto’s self-consistency analysis [2] or perhaps even OA theory [49])<sup>1</sup> to derive expressions for  $K_1$ ,  $K_2$ , and hopefully some results on the stability of the static async state too.

But it’s not clear how this can be done. Take finding  $K_1$ , the point at which async destabilizes. For the Kuramoto model, this is derived by exploiting the fact that in the sync state, the (nonidentical) oscillators split into two groups, one locked at fixed points  $\theta_i^*(\omega_i)$  with density  $\rho_{\text{locked}}(\theta)$ , the other drifting  $|\dot{\theta}_i| > 0$  with  $\rho_{\text{drift}}(\theta)$ . Skipping over details [2], the key to the analysis is  $\rho_{\text{drift}}(\theta)$  cancels out and that  $\rho_{\text{locked}}(\theta)$  has a simple form since it represents oscillators sitting at fixed points. For the swarmalator model, however, swarmalators are identical and, posttransition, *nonstationary*. This implies that they have a common  $\rho(x, \theta)$  (since they are identical) and that the form of  $\rho(x, \theta)$  cannot be easily guessed (since they are nonstationary). So Kuramoto’s trick cannot be straightforwardly adapted.

Blocked by these mathematical walls, we took the natural back path of divide and conquer: we split the swarmalator model into its radial and angular components; if the original model in Cartesian coordinates has the form  $(\dot{x}_i, \dot{y}_i, \dot{\theta}_i)$ , the phase being  $\theta_i$ , then the radial component of the model is  $(\dot{r}_i, \dot{\phi}_i)$ , and the angular  $(\dot{\phi}_i, \dot{\theta}_i)$ , where  $(r, \phi)$  are polar coordinates. The essence of the angular piece is especially simple (see the Appendix):

$$\dot{\phi}_i = \omega(r_i) + \frac{1}{N} \sum_j^N J(r_i, r_j) \sin(\phi_j - \phi_i) \cos(\theta_j - \theta_i), \quad (1)$$

$$\dot{\theta}_i = v(r_i) + \frac{1}{N} \sum_j^N K(r_i, r_j) \sin(\theta_j - \theta_i) \cos(\phi_j - \phi_i). \quad (2)$$

It is a pair of Kuramoto models where now the natural frequencies and couplings depend on the  $r_i, r_j$ , and the familiar

<sup>1</sup>OA theory is the theory based on the breakthrough work by Edward Ott and Tom Antonsen [49], who discovered an invariant manifold in density space for the Kuramoto model.

\*Corresponding author: [hhong@jbnu.ac.kr](mailto:hhong@jbnu.ac.kr)

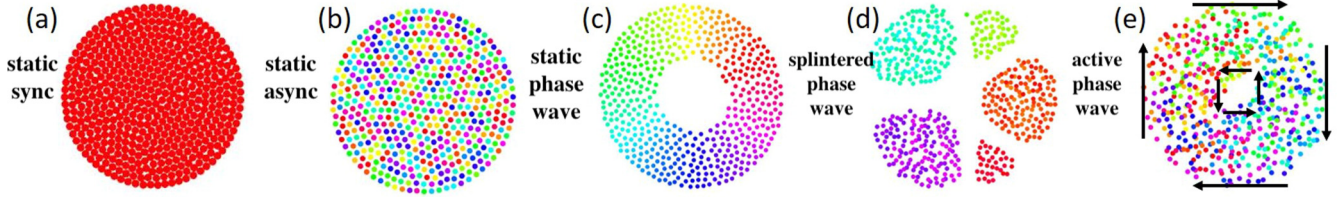


FIG. 1. Collective states of the 2D swarmalator model (defined in the Appendix) where swarmalators are represented as colored dots where the color refers to the swarmalators' phases. In all panels an Euler method was used with time step  $dt = 0.1$  for  $T = 1000$  units for  $N = 1000$  swarmalators. (a) Static sync  $(J, K, \sigma) = (1, 1, 10)$ , (b) static async  $(J, K, \sigma) = (1, 1, 10)$ , (c) static phase wave  $(J, K, \sigma) = (1, 1, 10)$ , (d) splintered phase wave  $(J, K, \sigma) = (1, 1, 10)$ , and (e) active phase wave. In the three static states (a–c) swarmalators do not move in space or phase. In the splintered phase wave, each colored chunk is a vortex: the swarmalators librate in both space and phase. In the active phase wave, the librations are excited into rotations; the swarmalators split into counterrotating groups as indicated by the black arrows. Figure adapted from [47].

sine terms are modified by cosines. The effect of the cosines is to make the sync position-dependent and the swarming phase-dependent—a lovely symmetry which captures the raw essence of swarmalators.

This emergence of this “ring model”<sup>2</sup> from the two-dimensional (2D) model got us excited. It hinted that the tools from sync studies might indeed be adapted for these new puzzles about swarmalators. The Kuramoto model with couplings distributed as  $K_i, K_j, K_{ij}$ , for example, has been solved exactly [50–54]—could we adapt these works to the ring model (since it has a similar form)?

This paper is the third in a series of papers which explore this tantalizing prospect. The strategy is to study the ring model piece by piece. First, we set the natural frequencies

and couplings at constants  $(\omega, \nu, J, K)$  [47]. Then we turned on quenched disorder in  $(\omega_i, \nu_i)$ , keeping  $(J, K)$  constant [48]. Here we isolate  $K_j$ -distributed couplings (defined in the model below) and keep the frequencies frozen at constants  $(\omega, \nu)$ . We discover several collective states, as well as generalizations of previously reported states, some of which we are able to analyze.

Last, we mention that the ring model with distributed  $K_j$  is worth studying in its own right, and not just as a warm up for the 2D swarmalator model. It is a toy model for the many natural swarmalators which move in quasi-one-dimensional (1D) rings such as vinegar eels and sperm [55–59]. Asymmetric couplings, as encoded by  $K_j$ , are common in such systems [60], yet are rarely studied.

## II. MODEL

The ring swarmalator model we study is

$$\dot{x}_i = \omega + \frac{1}{N} \sum_j J_j \sin(x_j - x_i) \cos(\theta_j - \theta_i), \quad (3)$$

$$\dot{\theta}_i = \nu + \frac{1}{N} \sum_j K_j \sin(\theta_j - \theta_i) \cos(x_j - x_i), \quad (4)$$

where  $(x_i, \theta_i) \in (S^1, S^1)$  are the position and phase of the  $i$ th swarmalator for  $i = 1, \dots, N$  and  $(\omega, \nu)$  and  $(J_j, K_j)$  are the associated natural frequencies and couplings. Notice we have switched  $\phi_i \rightarrow x_i$  to make it clear that  $x_i$  denotes an angle in space, as opposed to an internal phase like  $\theta$ . We set  $(\omega, \nu) = (0, 0)$  via a change of frame without loss of generality (wlog). As for the  $J_j, K_j$ , we derive most of our results for arbitrary distributions  $g(J), h(K)$ , but we use a simpler “double delta” distribution

$$g(J) = \delta(J - 1), \quad (5)$$

$$h(K) = p\delta(K - K_p) + (1 - p)\delta(K - K_n), \quad (6)$$

where  $K_p > 0$  and  $K_n < 0$  and  $0 \leq p \leq 1$ , as a working example throughout.

<sup>2</sup>We call this a “ring” model because when the radial dynamics are frozen, swarmalators' spatial motion is purely rotational; they move in rings. Of course, the radius of these rings will be different for each swarmalator, i.e.,  $r_i \neq r_j$ , so we could call it the “annular model.” However, the “ring” seems clearer to us and is consistent with the model Eq. (3) and Eq. (4) we study here in which the swarmalators do indeed run on a single ring.

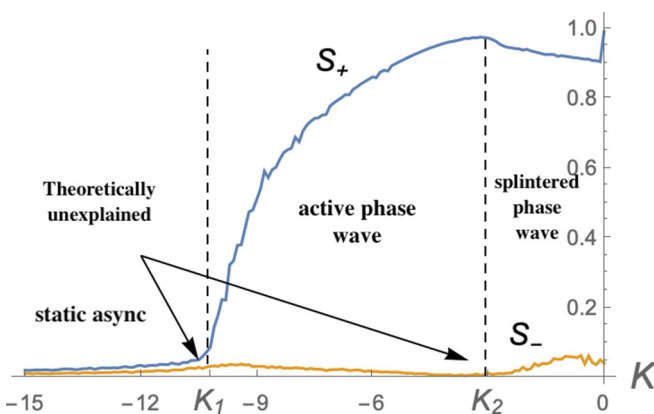


FIG. 2. Order parameters of the 2D swarmalator model (see the Appendix)  $S_{\pm} e^{i\Phi_{\pm}} := (N)^{-1} \sum_j e^{i(\phi_j \pm \theta_j)}$ , where  $\phi, \theta$  are the spatial angle and phase of swarmalators. The static sync state exists for  $K > 0$ , and the static phase wave for  $K = 0$  (these two states are not labeled in the figure to avoid overcrowding).

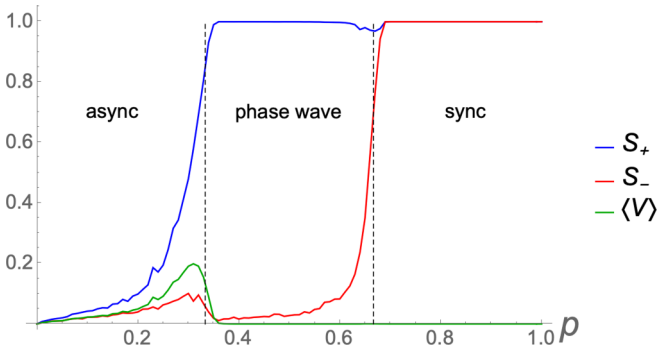


FIG. 3. Order parameters  $S_{\pm}$  and  $V$  vs  $p$  for  $Q = 2$  with  $Q = -K_n/K_p$ . The  $p_c$  and  $p_s$  are given by Eq. (17) and Eq. (49), respectively. Simulation parameters: RK4 with  $(dt, T, N) = (0.01, 1000, 1600)$ . Data points are averaged over 20 samples. For  $p_s \leq p \leq p_c$ , the buckled phase wave is realized for finite  $N$  for which  $S_- > 0$ . As  $N \rightarrow \infty$ , the buckle disappears, and the static phase wave is realized in which  $S_- = 0$ . We assume  $S_+ > S_-$  wlog. For  $p < p_s$  and finite  $N$ , the active async state occurs with  $V > 0$ . As  $N \rightarrow \infty$ ,  $V \rightarrow 0$  and the static async state is born.

### III. NUMERICS

We use two order parameters to catalog our models macroscopic behavior:

$$W_{\pm} = S_{\pm} e^{i\Phi_{\pm}} \equiv \frac{1}{N} \sum_{j=1}^N e^{i(x_j \pm \theta_j)}, \quad (7)$$

$$V = \frac{1}{N} \sum_{j=1}^N \left\langle \sqrt{\dot{x}_j^2 + \dot{\theta}_j^2} \right\rangle_t. \quad (8)$$

The  $S_{\pm}$  “rainbow order parameters”—so-called since they are maximal in the rainbow-like static phase wave state [Fig. 1(c)]—measure the global space-phase order. They are

maximal  $S_{\pm} = 1$  when  $x_i = \pm\theta_i + C$  for some constant  $C$ . They are minimal  $S_{\pm} = 0$  when  $x_i$  and  $\theta_i$  are uncorrelated. These order parameters arise naturally in the ring swarmalator model [29] and can distinguish between most of the model’s emergent states. They are blind, however, to the swarmalators’ motion. So we use the mean velocity  $V$  to detect if a collective state exists in which swarmalators are moving.

We numerically integrated the governing equations using an RK4 method and found five collective states (Supplemental Movie 1 [61]). Figure 3 plots  $S(p)$ ,  $V(p)$ , which demarcates the states. Code used for simulations is available at [62]. The states are the following:

*Static sync* for  $p > p_c$ :  $(x_i, \theta_i) = (x^*, \theta^*)$ . A “ $\pi$  state” where  $(x_i, \theta_i) = (x^*, \theta^*) \cup (x^* + \pi, \theta^* + \pi)$  also exists [47]. We call them both static sync. Here  $S_{\pm} = 1$  and  $V = 0$  [Figs. 4(a) and 4(e)].

*Static phase wave* for  $p_0 < p < p_c$ :  $x_i = \theta_i \pm C$  (the  $\pm$  refers to a clockwise or counterclockwise phase wave). Here either  $(S_+, S_-) = (1, 0)$  or  $(0, 1)$  (depending on the  $\pm$ ) and  $V = 0$ . Realized as  $N \rightarrow \infty$  [Figs. 4(b) and 4(f)].

*Buckled phase wave* near  $p_c$ : A static phase wave with a “buckle” so  $S_+ \approx 1$ ,  $S_- = 0$ ,  $V = 0$ . Realized for finite  $N$  [Figs. 4(c) and 4(g)].

*Noisy phase wave* for  $p < p_s$ : the static phase wave destabilizes into noisy, unsteady phase waves with  $V > 0$ . For  $p$  near  $p_c$ , there is approximate shear flow [Fig. 5(a)] similar to the active phase wave of the 2D model [Fig. 1(c)]. Here, however, the space correlation between  $x_i \approx \theta_i$  fluctuates as illustrated by the noisy  $S_{\pm}$  time series [Fig. 5(c)] where  $S_+ > 1$ ,  $S_- \approx 0$ . Realized for finite  $N$ .

*Async* for  $p \approx 0$ : For smaller  $p$ , the shear flow degenerates into erratic gaslike motion [Fig. 5(b)] with both  $S_+$ ,  $S_-$  noisy [Fig. 5(d)], which we call “active async.” Bands of sync’d swarmalators spontaneously appear and disappear (best viewed in Supplemental Movie 1 [61]). As  $p \rightarrow 0$ ,  $S_{\pm}$ ,  $V \rightarrow 0$  gradually decline, indicating the system becomes

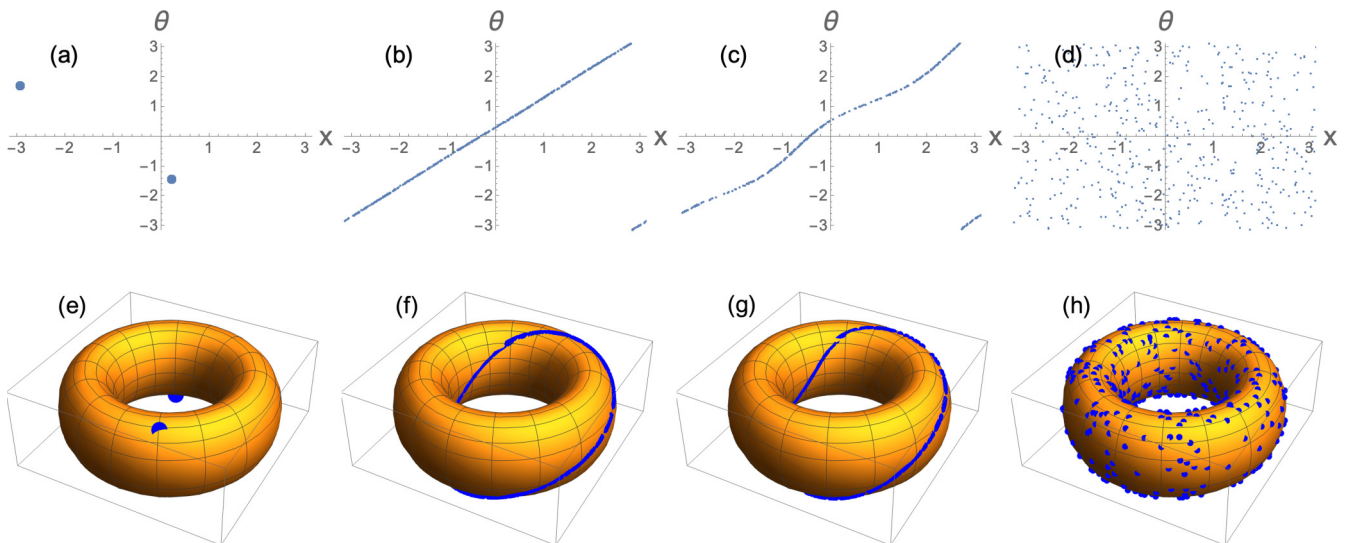


FIG. 4. Static collective states as scatter plots in  $(x, \theta)$  plane (top row) and plotted on a torus (bottom row) with dimensions  $(x, \theta)$ . (a, e) Static sync,  $(p, K_p, K_n) = (0.3, -0.5, 2)$ ; (b, f) static phase wave,  $(p, K_p, K_n) = (0.9, -0.5, 2)$ ; (c, g) buckled phase wave,  $(p, K_p, K_n) = (0.5, 1, -1.5)$ ; (d, h) static async,  $(p, K_p, K_n) = (0.85, 2, -10)$ . Simulation parameters: RK4 method with  $(dt, T, N) = (0.1, 100, 500)$ . In (c),  $N = 300$ . In (a), the point sizes have been enlarged to make things clearer.

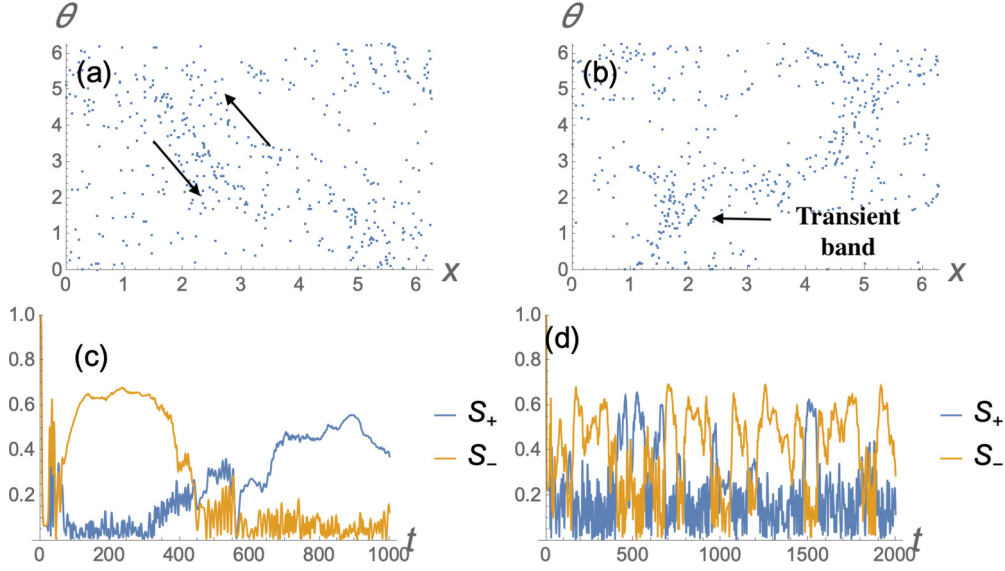


FIG. 5. Unsteady collective states. Top row, scatter plots in  $(x, \theta)$  space. Bottom row, time series of order parameters. (a–c) Swarmalators execute shear flow as indicated by the black arrows, like in the active phase wave on the 2D swarmalators model, but now  $S_{\pm}$  have noisy oscillations. Here  $(p, K_p, K_n) = (0.3, 1, -2)$  (b–d). Swarmalators execute erratic gaslike motion with  $S_{\pm}$  both noisy and similar magnitude. Bands of ordered swarmalators spontaneously appear and then disappear. Here  $(p, K_p, K_n) = (0.45, 5, -7)$  (best viewed in Supplemental Movie 1 [61]). Simulation parameters:  $(dt, T, N) = (0.25, 2000, 500)$ .

fully incoherent. Strangely, for all finite  $N$  we probed (up to  $10^4$  swarmalators) the async state is “active” with small but finite mean velocity  $V > 0$ . In the continuum limit  $N \rightarrow \infty$ , however, the state becomes truly static,  $V = 0$  (we prove this later).

#### IV. ANALYSIS

##### A. Static sync

Here swarmalators sit at fixed points:  $(x_i, \theta_i) = (x^*, \theta^*)$ . The  $\pi$  state, in which swarmalators split into two groups, one at  $(x^*, \theta^*)$ , the other at  $(x^* + \pi, \theta^* + \pi)$ , is dynamically equivalent to the single-cluster state because the governing ODEs are invariant under the “ $\pi$  transformation”  $x, \theta \rightarrow x + \pi, x + \pi$  [48]. So we analyze the one-cluster state in which  $(x_i, \theta_i) = (x^*, \theta^*)$  without loss of generality (wlog).

Now we derive the stability of this state for arbitrary  $g(J), h(K)$ . Linearizing Eqs. (3) and (4) about this fixed point yields

$$\begin{bmatrix} \dot{x}_i \\ \dot{\theta}_i \end{bmatrix} = M \begin{bmatrix} x_i \\ \theta_i \end{bmatrix}, \quad (9)$$

where the Jacobian  $M$  for the static sync at this fixed point has a block structure:

$$M = \frac{1}{N} \begin{bmatrix} A & 0 \\ 0 & B \end{bmatrix}, \quad (10)$$

where

$$A := \begin{bmatrix} -\sum_{j \neq 1} J_j & J_2 & \dots & J_N \\ J_1 & -\sum_{j \neq 2} J_j & \dots & J_N \\ \vdots & \vdots & \ddots & \vdots \\ J_1 & J_2 & \dots & -\sum_{j \neq N} J_j \end{bmatrix} \quad (11)$$

and

$$B := \begin{bmatrix} -\sum_{j \neq 1} K_j & K_2 & \dots & K_N \\ K_1 & -\sum_{j \neq 2} K_j & \dots & K_N \\ \vdots & \vdots & \ddots & \vdots \\ K_1 & K_2 & \dots & -\sum_{j \neq N} K_j \end{bmatrix}. \quad (12)$$

The matrices  $A$  and  $B$  have been studied before [29]. Their eigenvalues are  $\lambda_A = 0, -\langle J \rangle$  and  $\lambda_B = 0, -\langle K \rangle$  with multiplicities  $1, N-1$  (the zero eigenvalues stem from the rotational symmetry in the model). The eigenvalues of  $M$  are the union of those of  $A$  and  $B$   $\lambda_M = \lambda_A \cup \lambda_B$ . This follows from  $M$ 's block structure:  $\det(M) = \det(A)\det(B)$ . Putting this together gives

$$\lambda_0 = 0 \quad (\text{w.m. } 2), \quad (13)$$

$$\lambda_1 = -\langle J \rangle \quad (\text{w.m. } N-1), \quad (14)$$

$$\lambda_2 = -\langle K \rangle \quad (\text{w.m. } N-1), \quad (15)$$

where *w.m.* denotes with multiplicity. Thus sync destabilizes when  $\langle K \rangle = 0$  or  $\langle J \rangle = 0$ , which, we recall, holds for *general*  $g(J), h(K)$ . For the double delta distribution working example [Eq. (6)],

$$\begin{aligned} \langle K \rangle &= pK_p + (1-p)K_n \\ &= K_p[p(1+Q) - Q], \end{aligned} \quad (16)$$

where  $Q \equiv -K_n/K_p$ . Setting this to zero gives the critical fraction of positively coupled swarmalators

$$p_c = \frac{Q}{1+Q}, \quad (17)$$

which echoes a previous result [37].

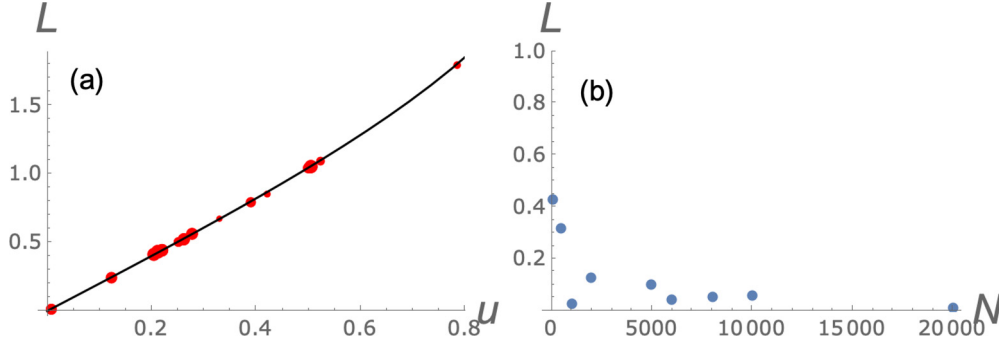


FIG. 6. (a) Black line, prediction Eq. (29); red dots, simulation parameters for  $(p, K_p, K_n) = (0.5, 1, -1.5)$ . Size of dots is proportional to the number of swarmalators  $N$ . Sim pars  $(dt, T) = (0.25, 1000)$  for  $N = 5, 10, \dots, 100$ . Any simulations for which the buckled phase wave was not realized were discarded. We asserted  $S_+ > S_-$  in simulations wlog for that  $U_+ > U_- \rightarrow u < 1$ . (b) Buckle size approaches 0 for large  $N$ .

### B. Buckled phase wave

For  $p < p_c$  and finite  $N$  the buckled phase wave is born. Here we derive the 1D manifold  $\Gamma(x, \theta) = 0$  which defines the state for arbitrary  $g(J), h(K)$  (the stability of the state is out of scope). First, we move to  $(\xi, \eta)$  coordinates:

$$\xi_i = x_i + \theta_i, \quad (18)$$

$$\eta_i = x_i - \theta_i. \quad (19)$$

The governing equations become

$$\begin{aligned} \dot{\xi}_i &= \frac{U_+}{2} \sin(\Psi_+ - \xi_i) + \frac{V_+}{2} \sin(\Theta_+ - \xi_i) \\ &+ \frac{U_-}{2} \sin(\Psi_- - \eta_i) - \frac{V_-}{2} \sin(\Theta_- - \eta_i), \end{aligned} \quad (20)$$

$$\begin{aligned} \dot{\eta}_i &= \frac{U_+}{2} \sin(\Psi_+ - \xi_i) - \frac{V_+}{2} \sin(\Theta_+ - \xi_i) \\ &+ \frac{U_-}{2} \sin(\Psi_- - \eta_i) + \frac{V_-}{2} \sin(\Theta_- - \eta_i), \end{aligned} \quad (21)$$

where

$$U_{\pm} e^{i\Psi_{\pm}} = \frac{1}{N} \sum_j J_j e^{i(x_j \pm \theta_j)}, \quad (22)$$

$$V_{\pm} e^{i\Theta_{\pm}} = \frac{1}{N} \sum_j K_j e^{i(x_j \pm \theta_j)} \quad (23)$$

are “glassy” order parameters [52]. Next, set Eq. (20) and (21) to zero since swarmalators are at fixed points. Then we add and subtract the equations to produce

$$0 = U_+ \sin \xi_i + U_- \sin \eta_i, \quad (24)$$

$$0 = V_+ \sin(\Theta_+ - \xi_i) - V_- \sin(\Theta_- - \eta_i), \quad (25)$$

where we set  $\Psi_{\pm} = 0$  wlog. Equations (24) and (25) are nullclines, curves in  $(\xi, \eta)$  space,  $\Gamma_1(\xi, \eta) = 0, \Gamma_2(\xi, \eta) = 0$ . Observe that the nullclines must (1) be identical and (2) describe the buckled phase wave  $\Gamma_1 = \Gamma_2 = \Gamma$ . Point 1 implies

$$\frac{U_-}{U_+} = \frac{V_-}{V_+}, \quad (26)$$

$$\Theta_+ - \Theta_- = \pi, \quad (27)$$

which we have confirmed numerically. Point 2 implies

$$\Gamma(\xi, \eta) = \sin \xi + u \sin \eta = 0, \quad (28)$$

where  $u := U_-/U_+$  and we have abused notation by using  $\Gamma$  for the curve in  $(\xi, \eta)$  space:  $\Gamma(\xi, \eta) \iff \Gamma(x, t)$ .

This is the desired parametrization of the buckled phase wave in terms of the glassy order parameters,  $U_{\pm}$ . We tested Eq. (28) as follows. Let the buckle be in the  $\xi$  direction wlog and define its size  $L := \max(\xi_i) - \min(\xi_i)$ . The buckle is symmetric about  $\xi = 0$  (really about  $\Psi_+ = \langle \xi \rangle$ , which we set to 0), so  $(\xi, \eta) = (\max(\xi_i) = L/2, \pi/2)$  lies on  $\Gamma$ . Then Eq. (28) implies

$$L = 2 \arcsin u. \quad (29)$$

We confirmed this prediction by simulating the system for various  $N$  and numerically computing  $u$  as depicted in Fig. 6(a).

We can compute  $u$  analytically as  $N \rightarrow \infty$  using Kuramoto’s self-consistency trick [2]. Figure 6(b), however, shows the buckle disappears as  $N \rightarrow \infty$  (the static phase wave is approached), which implies  $(U_+, U_-) = (1, 0) \Rightarrow u = 0$ ; so the calculation is in a sense moot. Nevertheless, we include it to show how the self-consistency calculation works for a density  $\rho(\xi, \eta)$  that is defined on compactly supported, non-trivial manifold  $\Gamma(\xi, \eta) = 0$  [as opposed to being defined on a fully supported space, like the density of oscillators  $\rho(\theta)$  of the Kuramoto model which lives on  $S^1$ ].

As  $N \rightarrow \infty$ , the expressions for the glassy order parameters become

$$\begin{aligned} U_+ &= \int_{\Gamma(\xi, \eta)} J \cos \xi \rho(\xi, \eta, J, K) \\ &\times g(J) h(K) d\xi d\eta dJ dK, \end{aligned} \quad (30)$$

$$\begin{aligned} U_- &= \int_{\Gamma(\xi, \eta)} J \cos \eta \rho(\xi, \eta, J, K) \\ &\times g(J) h(K) d\xi d\eta dJ dK, \end{aligned} \quad (31)$$

$$\Gamma(\xi, \eta, u) := \sin \xi + u \sin \eta = 0, \quad (32)$$

where we have set  $\Psi_{\pm} = 0$  wlog (which means the integrands  $e^{i\xi}, e^{i\eta} \rightarrow \cos \xi, \cos \eta$ ) and  $\rho(\xi, \eta, J, K)$  is the density of swarmalators in the Eulerian sense. Equation (32) repeats the definition of  $\Gamma(\xi, \eta, u)$  for convenience and explicitly denotes its dependence on  $u$ .

Notice in contrast to the self-consistency equations for the regular Kuramoto order parameter [2] that the inte-

grals above are *contour* integrals over  $\Gamma(x, \theta, u)$ . And, crucially,  $\Gamma(\xi, \eta, u)$  depends on  $u$ . So Eqs. (30)–(32) are a set of self-consistency equations for *four* quantities:  $U_+, U_-, \rho(\xi, \eta, J, K), \Gamma(\xi, \eta, u)$ —quite a challenge! Let's break them down. Recall that the contour integral of a function  $f(x, y)$  over a curve  $\delta(s)$  is

$$I = \int_{\delta} f(x, y) ds, \quad (33)$$

$$I = \int_{s_1}^{s_2} g(s) \sqrt{1 + \delta'(s)^2} ds, \quad (34)$$

where  $g(s) := f(x(s), y(s))$  is the function evaluated along the contour  $\delta(s)$  which has extremal points  $(s_1, s_2)$ . Now we apply this definition to Eqs. (30) and (31). First, we need an expression for the contour:  $\Gamma(\xi, \eta, u) \iff \gamma(s) := \arcsin u \sin(s)$  where we have chosen  $s := \eta$  as the active parameter which runs from  $[-\pi, \pi]$ . The line measure is  $\sqrt{1 + \gamma'(s)^2} = \sqrt{1 + \frac{u^2 \cos^2(s)}{1 - u^2 \sin^2(s)}}$ . Then Eqs. (30) and (31) become

$$U_+ = \int_{-\pi}^{\pi} J \cos \xi(s) \sqrt{1 + \frac{u^2 \cos^2(s)}{1 - u^2 \sin^2(s)}} \hat{\rho}(s, J, K) ds d\hat{J} d\hat{K}, \quad (35)$$

$$U_- = \int_{-\pi}^{\pi} J \cos \eta(s) \sqrt{1 + \frac{u^2 \cos^2(s)}{1 - u^2 \sin^2(s)}} \hat{\rho}(s, J, K) ds d\hat{J} d\hat{K}, \quad (36)$$

where  $\cos \xi(s) = \sqrt{1 - u^2 \sin^2 s}$  is found from the definition of the contour  $\sin \xi + u \sin \eta$ ,  $\hat{\rho}(s) := \rho(\xi(s), \eta(s))$  is the (unknown) density along the contour  $\gamma(s)$ , and we have defined  $(d\hat{J}, d\hat{K}) := (g(J)dJ, h(K)dK)$  for clarity. Recall  $u := U_-/U_+$ , so Eqs. (35) and (36) are a pair of self-consistency equations for  $(U_-, U_+, \hat{\rho})$ . Recall also that these are valid for arbitrary  $g(J), h(K)$ .

In principle, the next step is to derive an expression for  $\hat{\rho}$  in terms of  $U_{\pm}$  by solving the continuity equation. This is a daunting task, beyond the scope of the current paper (it's hard to do for the regular PDEs encountered in fluid mechanics, never mind the integro-PDE we are dealing with; we have an integro-PDE piece because the mean-field coupling imposes nonlocality in the velocity  $v$ ). In practice, we guess an ansatz for  $\hat{\rho}$ .

Numerics indicate that such an ansatz is a uniform density  $\hat{\rho}(s, J, K) = C^{-1}$  where  $C$  is a normalization constant.<sup>3</sup> Let's find  $U_-$ . Observe that the line measure  $\frac{u^2 \cos^2(s)}{1 - u^2 \sin^2(s)}$  in the integrand is symmetric and positive definite about 0, so when integrated against  $\cos(s)$ , as in Eq. (36), we get  $U_- = 0$ . This then trivializes the calculation for  $U_+$ . If  $U_- = 0$ , then  $u \rightarrow 0$  (assuming  $U_+ > 0$  so denominator is not zero) and Eq. (35)

reduces to  $U_+ = 1$ . Thus,

$$U_+ = 1, \quad (37)$$

$$U_- = 0. \quad (38)$$

To recap, we have proved that if the density along the contour  $\Gamma(\xi, \eta)$  is uniform  $\hat{\rho} = C$ , then  $(U_-, U_+) = (0, 1)$ , which means the contour is a straight line  $\Gamma(\xi, \eta) = \xi - \Psi_+ = 0$  where we have reinserted  $\Psi_+$  for clarity [remember that we set  $\Psi_+ = 0$  wlog just under Eq. (25)].<sup>4</sup> In other words, we are in the static phase wave, as we anticipated at the start of the calculation.

### C. Static phase

Numerics suggest that this state is unstable for all finite  $N$ . We were, however, unable to prove this. For the finite case, disordered  $K_j$  made finding the eigenvalues of the associated Jacobian too difficult (for constant couplings, the eigenvalues were findable for all finite  $N!$  [47]). For the infinite case, the density of the state is a delta function  $\rho(\xi, \eta) = (2\pi)^{-1} \delta(\xi - C)$  or  $(2\pi)^{-1} \delta(\eta - C)$ , which is difficult to perturb around. So, instead, we numerically computed the eigenvalues for various  $N$ , which confirmed the state was unstable. We hope future researchers will provide a rigorous proof.

We do, however, have a trivial result for the glassy order parameters. Assuming the clockwise phase wave  $(S_+, S_-) = (1, 0)$  and the double delta coupling distribution, we get

$$V_+ = \langle K e^{i\xi} \rangle = \langle K \rangle, \quad (39)$$

$$V_+ = p(K_1 - K_2) + K_2, \quad (40)$$

which agrees with simulation. The other order parameters are trivial:  $V_- = U_- = 0$  and  $U_+ = 1$ .

### D. Static async

In the  $N \rightarrow \infty$  limit this state is given by  $\rho(\xi, \eta, K, J, t) = (4\pi^2)^{-1}$ . The density obeys the continuity equation

$$\dot{\rho} + \nabla \cdot (v\rho) = 0, \quad (41)$$

where the velocity  $v$  is given by Eqs. (20) and (21) and is interpreted in the Eulerian sense. Consider the perturbation

$$\rho = \rho_0 + \epsilon \rho_1 = (4\pi^2)^{-1} + \epsilon \rho_1(\xi, \eta, J, K, t). \quad (42)$$

We substitute this perturbation into the continuity equation, expand  $\rho_1$  in a Fourier series,

$$\rho_1(\xi, \eta, J_+, J_-, t) = c_+(J_+, J_-, t) e^{-i\xi} + c_-(J_+, J_-, t) e^{-i\eta} + \text{c.c.} + \rho_1^\dagger(\xi, \eta, J_+, J_-, t), \quad (43)$$

where  $J_{\pm} = (J \pm K)/2$  and  $\rho_1^\dagger$  contains all the higher harmonics, and collect the ODEs for each mode. The result is

$$\dot{c}_{\pm} = \frac{1}{2} \int \hat{J}_+ c_{\pm}(\hat{J}_+, \hat{J}_-, t) h(\hat{J}_+) h(\hat{J}_-) d\hat{J}_+ d\hat{J}_-. \quad (44)$$

Seeking the discrete spectrum  $c = e^{\lambda t} b(\hat{J}_+, \hat{J}_-)$  we eventually find

$$\lambda = \frac{\langle J_+ \rangle}{2}. \quad (45)$$

<sup>3</sup>Note that the dependence on  $(J, K)$  drops out. There are two ways to interpret this. First, is to assume that at every  $s$  there is a full distribution of swarmalators with  $g(J), h(K)$ . In other words, the mass of  $\rho$  is spread out evenly over its arguments  $(s, J, K)$  supported on  $[-\pi, \pi] \times R \times R$ . Second, we can interpret  $\hat{\rho}(s, J, K)$  as the average over many distributions of  $(J, K)$ .

<sup>4</sup> $\Phi_+$  is determined by the initial condition and can be 0 wlog because of the rotational symmetry of the model.

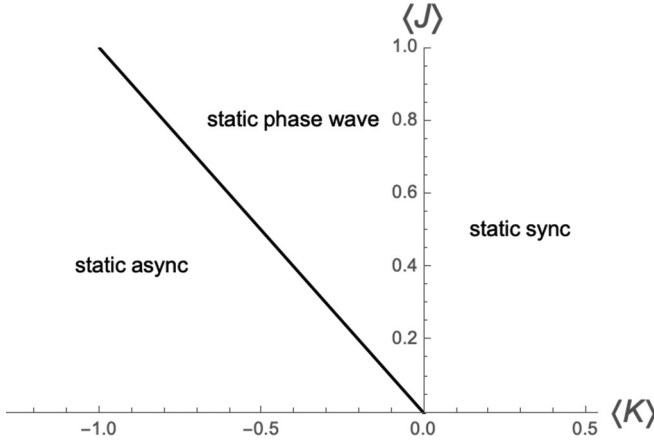


FIG. 7. Bifurcation diagram in  $(\langle J \rangle, \langle K \rangle)$  space in the  $N \rightarrow \infty$  limit valid for arbitrary coupling distributions  $g(J), h(K)$ .

Setting  $\lambda = 0$  then yields

$$\langle J_+ \rangle = 0, \quad (46)$$

$$\langle J \rangle + \langle K \rangle = 0, \quad (47)$$

$$\langle K \rangle_c = -\langle J \rangle, \quad (48)$$

which generalizes the finding in [47]. This is for general distributions  $f(J), h(K)$ . For the double delta working example this becomes

$$p_s = \frac{1 + K_n}{K_n - K_p}. \quad (49)$$

This completes our analysis. Figure 7 reports the bifurcation diagram in  $(\langle J \rangle, \langle K \rangle)$  space, which is valid as  $N \rightarrow \infty$  and for *arbitrary* coupling distributions  $g(K), h(K)$ . It is a clean generalization of the identical coupling limit in [47] where the couplings are replaced by their mean values  $J, K \rightarrow \langle J \rangle, \langle K \rangle$ .

## V. OTHER COUPLING DISTRIBUTIONS

We ran simulations for three other coupling distributions:

- (1) Single Gaussian:  $h(K) = N(\mu, \sigma|K)$
- (2) Mixed Gaussian:  $h(K) = pN(K_1, \sigma|K) + (1 - p)N(K_2, \sigma|K)$
- (3) Triple delta:  $h(K) = p_1\delta(K - K_1) + p_2\delta(K - K_2) + p_3\delta(K - K_3)$

where  $N(\mu, \sigma|x)$  is the normal distribution for random variable  $x$ . We found the same states in each case. Figure 8 summarizes this by plotting the order parameters, which have the same structure as the double delta model.

## VI. DISCUSSION

The ring model is intended as a stepping stone to the 2D swarmalator model. Previous work showed constant couplings produced 1D analogs of the static sync, static phase wave, and static async states [47], while distributed  $(v_i, \omega_i)$  produced a 1D active phase wave [48]. We were hoping  $K_j$  couplings might produce a 1D splintered phase wave (specifically, a statistically stationary, and thus analyzable, 1D analog).

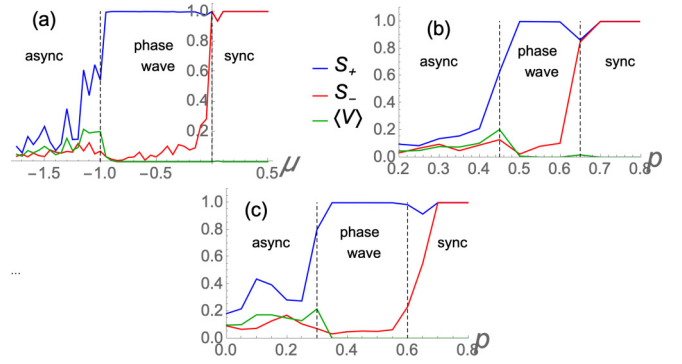


FIG. 8. Order parameters for different coupling distributions. The same structure is observed for (a) Gaussian with  $\sigma = 1$ , (b) mixture of Gaussians with  $(K_p, K_n, \sigma) = (-2, 1, 0.35)$ , and (c) triple delta with  $(p_1, p_2, p_3) = (p, (1 - p)/2, (1 - p)/2)$  and  $(K_1, K_2, K_3) = (1, 0.25, -4)$ . Simulation parameters are  $(dt, T, N) = (0.5, 500, 300)$ .

This wasn't the case. For infinite  $N$ , we found the same physics as the constant coupling model: the self-same static states cropped up. Moreover, the critical couplings were simply promoted to averages; the sync boundary became  $(J > 0, K > 0) \rightarrow (\langle J \rangle > 0, \langle K \rangle > 0)$ , the static async  $J_+ < 0 \rightarrow \langle J_+ \rangle < 0$  [recall, though, that these results hold for arbitrary  $g(J), h(K)$ ]. Still, this negative result is useful. It tells us that  $K_j$  is not the mechanism behind the nonstationarity in the splintered phase wave. Our next work will investigate if  $K_i$ -type couplings [where the  $K_i$  sits outside the sum in Eq. (3) and (4)] will produce a 1D splintered phase wave.

Recall that for finite  $N$ , however, the  $K_j$  couplings *did* produce alternative physics: a noisy phase wave and an active async state. The shear flow in the noisy phase wave imitates the flow in real-world swarmalators such as sperm [58] and vinegar eels [8,9] which spontaneously form counterrotating phases waves when confined to quasi-1D rings. The interesting part (to us at least) is that the noisy behavior occurs for *identical* swarmalators; the fluctuations arise from neither heterogeneous natural frequencies nor external sources, as one might expect. Rather, they are generated from the interactions between the internal and external degrees of freedom (phases  $\theta_i$  and positions  $x_i$  respectively). As for the active async state, the transient cluster formation was not seen in the constant coupling model and is reminiscent of the cluster dynamics in recent experiments of synthetic microswimmers [57] (these cluster dynamics are best viewed in Supplemental Movie 1 [61]).

Opportunities for future work include adding delayed interactions, external forcing, or heterogeneous natural frequencies. A proof for the stability of the static phase wave (see Sec. IV C) would also be interesting.

## ACKNOWLEDGMENT

This research was supported by the NRF Grant No. 2021R1A2B5B01001951 (H.H.).

## APPENDIX: CONNECTION OF RING MODEL TO 2D SWARMALATOR MODEL

Here we show how the ring model is contained within the 2D swarmalator model, which is given by

$$\dot{\mathbf{x}}_i = \mathbf{v}_i + \frac{1}{N} \sum_{j=1}^N [\mathbf{I}_{\text{att}}(\mathbf{x}_j - \mathbf{x}_i)F(\theta_j - \theta_i) - \mathbf{I}_{\text{rep}}(\mathbf{x}_j - \mathbf{x}_i)], \quad (\text{A1})$$

$$\dot{\theta}_i = \omega_i + \frac{K}{N} \sum_{j=1}^N H_{\text{att}}(\theta_j - \theta_i)G_{\sigma}(\mathbf{x}_j - \mathbf{x}_i). \quad (\text{A2})$$

In [29], the choices  $I_{\text{att}} = x/|x|$ ,  $I_{\text{rep}} = x/|x|^2$ ,  $F(\theta) = 1 + J \cos(\theta)$ ,  $G(x) = 1/|x|$ ,  $H_{\text{att}}(\theta) = \sin(\theta)$  were made. However, choosing linear spatial attraction  $I_{\text{att}}(x) = x$ , inverse square spatial repulsion  $I_{\text{rep}}(x) = x/|x|^2$ , and truncated parabolic space-phase coupling  $G(x) = (1 - |x|^2/\sigma^2)H_{\text{heaviside}}(\sigma - |x|)$ :

$$\dot{\mathbf{x}}_i = \frac{1}{N} \sum_{j \neq i}^N \left\{ \mathbf{x}_j - \mathbf{x}_i [1 + J \cos(\theta_j - \theta_i)] - \frac{\mathbf{x}_j - \mathbf{x}_i}{|\mathbf{x}_j - \mathbf{x}_i|^2} \right\}, \quad (\text{A3})$$

$$\dot{\theta}_i = \frac{K}{N} \sum_{j \neq i}^N \sin(\theta_j - \theta_i) \left( 1 - \frac{|\mathbf{x}_j - \mathbf{x}_i|^2}{\sigma^2} \right) H_{\text{heaviside}}(\sigma - |\mathbf{x}_j - \mathbf{x}_i|) \quad (\text{A4})$$

gives the same qualitative behavior but is nicer to work with analytically (see the Appendix in [47])

The ‘‘linear parabolic’’ model, so called because  $I_{\text{att}} = x$  and  $G(x)$  is a parabolic, is cleaner analytically. In polar coordinates it takes the form

$$\dot{r}_i = H_r(r_i, \phi_i) - Jr_i R_0 \cos(\Psi_0 - \theta_i) + \frac{J}{2} \{ \tilde{S}_+ \cos[\Phi_+ - (\phi_i + \theta_i)] + \tilde{S}_- \cos[\Phi_- - (\phi_i - \theta_i)] \},$$

$$\dot{\phi}_i = H_{\phi}(r_i, \phi_i) + \frac{J}{2r_i} \{ \tilde{S}_+ \sin[\Psi_+ - (\phi_i + \theta_i)] + \tilde{S}_- \sin[\Psi_- - (\phi_i - \theta_i)] \},$$

$$\dot{\theta}_i = K \left( 1 - \frac{r_i^2}{\sigma^2} \right) R_0 \sin(\Phi_0 - \theta_i) - \frac{K}{\sigma^2} R_1 \sin(\Phi_1 - \theta_i) + \frac{K r_i}{\sigma^2} \{ \tilde{S}_+ \sin[\Psi_+ - (\phi_i + \theta_i)] - \tilde{S}_- \sin[\Psi_- - (\phi_i - \theta_i)] \},$$

where

$$H_r(r_i, \phi_i) = \frac{1}{N} \sum_j [r_j \cos(\phi_j - \phi_i) - r_i] (1 - d_{ij}^{-2}), \quad (\text{A5})$$

$$H_{\phi}(r_i, \phi_i) = \frac{1}{N} \sum_j \frac{r_j}{r_i} \sin(\phi_j - \phi_i) (1 - d_{ij}^{-2}), \quad (\text{A6})$$

$$Z_0 = R_0 e^{i\Psi_0} = \frac{1}{N} \sum_j e^{i\theta_j}, \quad (\text{A7})$$

$$\hat{Z}_0 = \hat{R}_0 e^{i\hat{\Psi}_0} = \frac{1}{N} \sum_{j \in N_i} e^{i\theta_j}, \quad (\text{A8})$$

$$Z_2 = R_2 e^{i\Psi_2} = \frac{1}{N} \sum_j r_j^2 e^{i\theta_j}, \quad (\text{A9})$$

$$\hat{Z}_2 = \hat{R}_2 e^{i\hat{\Psi}_2} = \frac{1}{N} \sum_{j \in N_i} r_j^2 e^{i\theta_j}, \quad (\text{A10})$$

$$\tilde{W}_{\pm} = \tilde{S}_{\pm} e^{i\Psi_{\pm}} = \frac{1}{N} \sum_j r_j e^{i(\phi_j \pm \theta_j)}, \quad (\text{A11})$$

$$\hat{W}_{\pm} = \hat{S}_{\pm} e^{i\hat{\Psi}_{\pm}} = \frac{1}{N} \sum_{j \in N_i} r_j e^{i(\phi_j \pm \theta_j)}, \quad (\text{A12})$$

where the  $\hat{Z}_0, \dots$  order parameters are summed over all the neighbors  $N_i$  of the  $i$ th swarmalator: those within a distance  $\sigma$ . Notice that rainbow order parameters  $\tilde{W}$  here are weighted by the radial distance  $r_j$ . Assuming  $\sigma > \max(d_{ij})$ , we can set  $\hat{Z}_0 = Z_0$ ,  $\hat{Z}_1 = Z_1$ ,  $\tilde{W}_{\pm} = W_{\pm}$ . Then  $S_{\pm} \sin[\Phi_{\pm} - (\phi \pm \theta)]$  and other parts of the ring model start to emerge. If we assume there is no global synchrony  $Z_0 = Z_2 = 0$ , which happens generically in the frustrated parameter regime  $K < 0, J > 0$ , and transform to  $\xi_i = \phi_i + \theta_i$  and  $\eta_i = \phi_i - \theta_i$  coordinates the ring model is revealed:

$$\dot{r}_i = \tilde{v}(r_i, \phi_i) + \frac{J}{2} [\tilde{S}_+ \cos(\Phi_+ - \xi_i) + \tilde{S}_- \cos(\Phi_- - \eta_i)], \quad (\text{A13})$$

$$\dot{\xi}_i = \tilde{\omega}(r_i, \phi_i) + [J_+(r_i) \tilde{S}_+ \sin(\Psi_+ - \xi_i) + J_-(r_i) \tilde{S}_- \sin(\Psi_- - \eta_i)], \quad (\text{A14})$$

$$\dot{\eta}_i = \tilde{\omega}(r_i, \phi_i) + [J_-(r_i) \tilde{S}_+ \sin(\Psi_+ - \xi_i) - J_+(r_i) \tilde{S}_- \sin(\Psi_- - \eta_i)], \quad (\text{A15})$$

where

$$\tilde{v}(r_i, \phi_i) = H_r(r_i, \phi_i), \quad (\text{A16})$$

$$\tilde{\omega}(r_i, \phi_i) = H_{\phi}(r_i, \phi_i), \quad (\text{A17})$$

$$J_{\pm}(r_i) = \frac{J}{2r_i} \pm \frac{K r_i}{\sigma^2}. \quad (\text{A18})$$



In the spirit of minimalism, we suppress the  $\phi_i$  dependence in the  $\nu$ ,  $\omega$  in our definition of the ring model in the main text.

Hence the reported ring model is the “essence” of the angular piece of the 2D model, as described.

- 
- [1] A. T. Winfree, *The Geometry of Biological Time*, Vol. 2 (Springer, New York, 1980).
- [2] Y. Kuramoto, *Chemical Oscillations, Waves, and Turbulence* (Courier Corporation, 2003).
- [3] A. Pikovsky, M. Rosenblum, and J. Kurths, *Self* **2**, 3 (2001).
- [4] W. Bialek, A. Cavagna, I. Giardina, T. Mora, E. Silvestri, M. Viale, and A. M. Walczak, *Proc. Natl. Acad. Sci. USA* **109**, 4786 (2012).
- [5] Y. Katz, K. Tunstrøm, C. C. Ioannou, C. Huepe, and I. D. Couzin, *Proc. Natl. Acad. Sci. USA* **108**, 18720 (2011).
- [6] Y. Yang, J. Elgeti, and G. Gompper, *Phys. Rev. E* **78**, 061903 (2008).
- [7] I. H. Riedel, K. Kruse, and J. Howard, *Science* **309**, 300 (2005).
- [8] A. Quillen, A. Peshkov, E. Wright, and S. McGaffigan, *Phys. Rev. E* **104**, 014412 (2021).
- [9] A. Quillen, A. Peshkov, E. Wright, and S. McGaffigan, *Soft Matter* **18**, 1174 (2022).
- [10] G. I. Taylor, *Proc. R. Soc. London A* **209**, 447 (1951).
- [11] S. L. Tamm, T. Sonneborn, and R. V. Dippell, *J. Cell Biol.* **64**, 98 (1975).
- [12] J. Yan, M. Bloom, S. C. Bae, E. Luijten, and S. Granick, *Nature (London)* **491**, 578 (2012).
- [13] S. Hwang, T. D. Nguyen, S. Bhaskar, J. Yoon, M. Klaiber, K. J. Lee, S. C. Glotzer, and J. Lahann, *Adv. Funct. Mater.* **30**, 1907865 (2020).
- [14] B. Zhang, A. Sokolov, and A. Snezhko, *Nat. Commun.* **11**, 1 (2020).
- [15] A. Bricard, J.-B. Caussin, D. Das, C. Savoie, V. Chikkadi, K. Shitara, O. Chepizhko, F. Peruani, D. Saintillan, and D. Bartolo, *Nat. Commun.* **6**, 7470 (2015).
- [16] B. Zhang, H. Karani, P. M. Vlahovska, and A. Snezhko, *Soft Matter* **17**, 4818 (2021).
- [17] R. K. Manna, O. E. Shklyae, and A. C. Balazs, *Proc. Natl. Acad. Sci. USA* **118**, e2022987118 (2021).
- [18] M. Li, M. Brinkmann, I. Pagonabarraga, R. Seemann, and J.-B. Fleury, *Commun. Phys.* **1**, 1 (2018).
- [19] K. Chaudhary, J. J. Juárez, Q. Chen, S. Granick, and J. A. Lewis, *Soft Matter* **10**, 1320 (2014).
- [20] A. Hrabec, V. Křížáková, S. Pizzini, J. Sampaio, A. Thiaville, S. Rohart, and J. Vogel, *Phys. Rev. Lett.* **120**, 227204 (2018).
- [21] E. Haltz, S. Krishnia, L. Berges, A. Mougin, and J. Sampaio, *Phys. Rev. B* **103**, 014444 (2021).
- [22] A. Barciś, M. Barciś, and C. Bettstetter, in *2019 International Symposium on Multi-Robot and Multi-Agent Systems (MRS)* (IEEE, 2019), pp. 98–104.
- [23] A. Barciś and C. Bettstetter, *IEEE Access* **8**, 218752 (2020).
- [24] J. D. Monaco, G. M. Hwang, K. M. Schultz, and K. Zhang, *Biol. Cybern.* **114**, 269 (2020).
- [25] D. Tanaka, *Phys. Rev. Lett.* **99**, 134103 (2007).
- [26] M. Iwasa and D. Tanaka, *Phys. Rev. E* **81**, 066214 (2010).
- [27] M. Iwasa, K. Iida, and D. Tanaka, *Phys. Rev. E* **81**, 046220 (2010).
- [28] M. Iwasa and D. Tanaka, *Phys. Lett. A* **381**, 3054 (2017).
- [29] K. P. O’Keeffe, H. Hong, and S. H. Strogatz, *Nat. Commun.* **8**, 1 (2017).
- [30] H. K. Lee, K. Yeo, and H. Hong, *Chaos* **31**, 033134 (2021).
- [31] H. Hong, *Chaos* **28**, 103112 (2018).
- [32] J. U. Lizarraga and M. A. de Aguiar, *Chaos* **30**, 053112 (2020).
- [33] K. P. O’Keeffe, J. H. M. Evers, and T. Kolokolnikov, *Phys. Rev. E* **98**, 022203 (2018).
- [34] S.-Y. Ha, J. Jung, J. Kim, J. Park, and X. Zhang, *Kinetic & Related Models* **14**, 429 (2021).
- [35] G. K. Sar, S. N. Chowdhury, M. Perc, and D. Ghosh, *New J. Phys.* **24**, 043004 (2022).
- [36] K. O’Keeffe and C. Bettstetter, *Micro-and Nanotechnology Sensors, Systems, and Applications XI* **10982**, 383 (2019).
- [37] H. Hong, K. Yeo, and H. K. Lee, *Phys. Rev. E* **104**, 044214 (2021).
- [38] U. Schilcher, J. F. Schmidt, A. Vogell, and C. Bettstetter, in *2021 IEEE International Conference on Autonomic Computing and Self-Organizing Systems (ACSOS)* (IEEE, 2021), pp. 90–99.
- [39] P. Japón, F. Jiménez-Morales, and F. Casares, *Cells Develop.* **169**, 203726 (2022).
- [40] V. Vijayan and P. P. Das, *arXiv:2202.02383* (2022).
- [41] K. Schultz, M. Villafane-Delgado, E. P. Reilly, G. M. Hwang, and A. Saksena, *arXiv:2103.08583* (2021).
- [42] J. Yan, S. C. Bae, and S. Granick, *Soft Matter* **11**, 147 (2015).
- [43] S. H. Strogatz, *Physica D* **143**, 1 (2000).
- [44] S. H. Strogatz and R. E. Mirollo, *J. Stat. Phys.* **63**, 613 (1991).
- [45] R. Mirollo and S. H. Strogatz, *J. Nonlinear Sci.* **17**, 309 (2007).
- [46] J. D. Crawford, *J. Stat. Phys.* **74**, 1047 (1994).
- [47] K. O’Keeffe, S. Ceron, and K. Petersen, *Phys. Rev. E* **105**, 014211 (2022).
- [48] S. Yoon, K. O’Keeffe, J. Mendes, and A. Goltsev, *arXiv:2203.10191* (2022).
- [49] E. Ott and T. M. Antonsen, *Chaos* **18**, 037113 (2008).
- [50] H. Hong and S. H. Strogatz, *Phys. Rev. E* **84**, 046202 (2011).
- [51] H. Hong and S. H. Strogatz, *Phys. Rev. E* **85**, 056210 (2012).
- [52] I. M. Kloumann, I. M. Lizarraga, and S. H. Strogatz, *Phys. Rev. E* **89**, 012904 (2014).
- [53] H. Hong, K. P. O’Keeffe, and S. H. Strogatz, *Phys. Rev. E* **93**, 022219 (2016).
- [54] H. Hong, K. P. O’Keeffe, and S. H. Strogatz, *Chaos: Interdisciplin. J. Nonlin. Sci.* **26**, 103105 (2016).
- [55] J. Yuan, D. M. Raizen, and H. H. Bau, *Proc. Nat. Acad. Sci.* **111**, 6865 (2014).
- [56] J. Yuan, D. M. Raizen, and H. H. Bau, *J. R. Soc. Interface.* **12**, 20150227 (2015).
- [57] S. Ketzetzi, M. Rinaldin, P. Dröge, J. de Graaf, and D. J. Kraft, *Nat. Comm.* **13**, 1772 (2022).
- [58] A. Creppy, F. Plouraboué, O. Praud, X. Druart, S. Cazin, H. Yu, and P. Degond, *J. R. Soc. Interface.* **13**, 20160575 (2016).
- [59] I. Aihara, T. Mizumoto, T. Otsuka, H. Awano, K. Nagira, H. G. Okuno, and K. Aihara, *Sci. Rep.* **4**, 3891 (2014).

- [60] B. Liebchen and A. K. Mukhopadhyay, *J. Phys.: Condens. Matter* **34**, 083002 (2022).
- [61] See Supplemental Material at <http://link.aps.org/supplemental/10.1103/PhysRevE.105.064208> for movie of collective states as scatter plots in the  $(x, \theta)$  plane. Simulation parameters: same as those described in text.
- [62] K. O'Keeffe, *Swarmalators*, <https://github.com/Khev/swarmalators/tree/master/1D/on-ring/mixed-coupling/kj>.